Dimorphism in Late Cretaceous ammonites— evidence from early Turonian ammonite faunas of the Brießnitz Formation in Saxony, Germany

CONSTANZE WONDREJZ, EMAD NAGM, and MARKUS WILMSEN

Systematic palaeontological and biometric-statistical analyses (classical clustering and linear discriminant analysis) of statistically significant populations of three early Turonian ammonite species from offshore marls of the Brießnitz Formation (Saxonian Cretaceous Basin, eastern Germany) were used to evaluate a formerly just visually suspected hypothesis of a size dimorphism within the taxa. The studied faunas can in fact be regarded as contemporaneous late early Turonian fossil assemblages derived from a palaeobiogeographic and depositional entity. However, only one of the three species passed the statistical tests. Neither in *Lewesiceras peramplum* nor in *Mammites nodosoides* can a dimorphism be proven. In both taxa, no other features than size can be recognised that differ significantly between the overlapping groups. Furthermore, adulthood cannot be proven due to the absence of unequivocal mature modifications. Thus, a combination of large intraspecific variability and commonly incompletely preserved (i.e., small) specimens dissembles dimorphic populations at a first glance. On the other hand, the suspected dimorphism in *Spathites* (*Jeanrogericeras*) *reveliereanus* was confirmed by the statistical analyses of numerous biometric parameters. Not only the maximum diameters but also the distinct apertural cross-sections and ornament show significant differences between the statistically clearly separated two groups. Furthermore, a decline in ornament and widening of the body chamber in fully grown macroconch specimens, regarded as a mature modification of the shell, demonstrate that the antidimorphs really differed in adult morphology. Thus, it can be shown that there are in fact two forms in the fossil assemblage of *S.* (*J.*) *reveliereanus* that, based on their morphological differences and lack of any overlap, represent micro- and macroconchs (inferred males and females) of an evidently dimorphic ammonite species. Finally, we conclude that simple visual inspection is commonly insufficient for the reliable proof of dimorphism in ammonoids.

Key words: Ammonitina, biometric-statistical analyses, dimorphic pairs, Elbtal Group, Cretaceous.

Constanze Wondrejz [conni.wondrejz@freenet.de], Dresden, Germany.
Emad Nagm [emad.nagm@yahoo.com; ORCID: https://orcid.org/0000-0003-0384-0446], Department of Geology, College of Science, Taibah University, Madinah 41411, Saudi Arabia and Department of Geology, Faculty of Science, Al-Azhar University, Assiut 71524, Egypt.
Markus Wilmsen [markus.wilmsen@senckenberg.de; ORCID: https://orcid.org/0009-0005-0076-8014] (corresponding author), Senckenberg Naturhistorische Sammlungen Dresden, Museum für Mineralogie und Geologie, Sektion Paläozoologie, Königsbrücker Landstr. 159, 01109 Dresden, Germany.

Introduction

The Ammonoidea are the largest subclass of the Cephalopoda, comprising 163 families. They range in age from the Early Devonian to the end of the Cretaceous and are one of the most important and iconic groups of fossils (Lehmann 1976). Even though they had a successful evolutionary and ecological history for over 300 million years of geological time, surviving at least three major mass extinction events, they received only little attention as potential useful monitor organisms of palaeoenvironmental conditions until late in the last century (House 1989; Tsujita and Westermann 1998; Ritterbush et al. 2014). Since then, the understanding of ammonoid palaeoecology increased with numerous studies about their functional morphology (e.g., Ward 1979; Elmi 1993; Westermann 1996; Tsujita and Westermann 1998). Today these molluscs are palaeontological model organisms
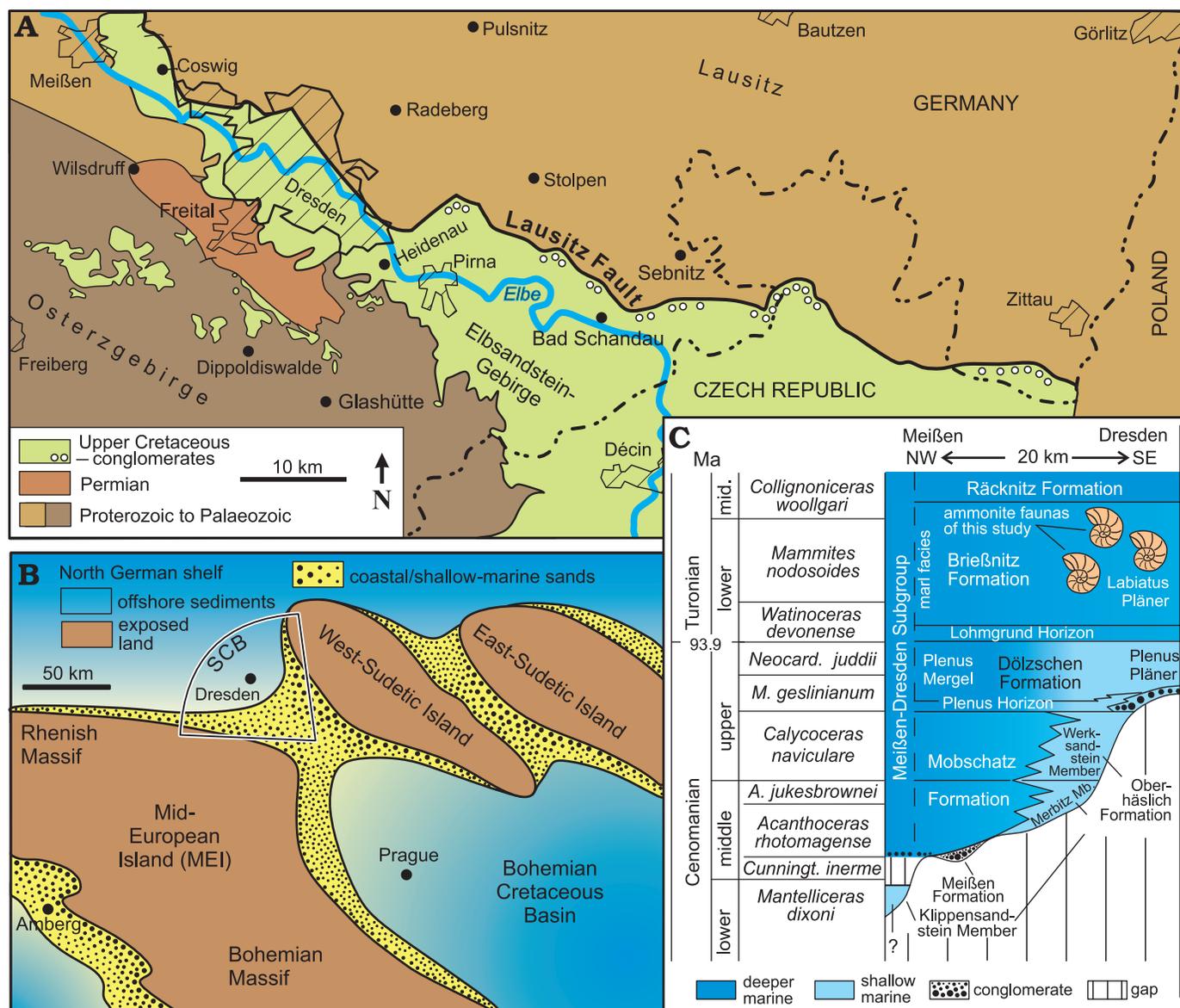
Fig. 1. Geological framework and stratigraphy of the lower Elbtal Group. **A**. Distribution of the Elbtal Group (green) in the area between Meißen and the German/Czech Republic border. **B**. Palaeogeographic setting of the Saxonian Cretaceous Basin (SCB). **C**. Chrono-, bio- and lithostratigraphy of the lower Elbtal Group in the area between Meißen and Dresden; the stratigraphic position of the ammonite faunas from the Brießnitz Formation is indicated. Supplemented and modified after Wilmsen et al. (2019, 2022) and Niebuhr et al. (2020). Abbreviations: *A.*, *Acanthoceras*; *Cunningt.*, *Cunningtoniceras*; *M.*, *Metoicoceras*; mid., middle; *Neocard.*, *Neocardioceras*.

for the study of diversity, biogeography, biostratigraphy, and macroevolution due to their high disparity and diversity, wide geographical distribution, and high evolutionary rates (Kennedy and Cobban 1976; Kennedy 1989; Landmann et al. 1996; Keupp 2000; Monnet et al. 2011; see also recent synopses on all these different ammonitological aspects in Klug et al. 2015a, b).

From a developmental point of view, a potential sexual dimorphism in ammonites can be characterised by two classes of individuals with a juvenile ontogeny that was identical up to a particular size (shell diameter). From a certain point in ontogeny, two different morphotypes developed, a macroconch (inferred female) and a microconch (inferred male); the opposing members of a dimorphic pair have also been called antidimorphs (Davis 1972). In some cases, the dimorphic correspondence between two morphs may be readily differentiated by direct visual inspection, but in general, statistical evaluations usually provide a higher support for the standard morphologic analysis (Parent and Zatoń 2016).

Even if it is still a debated topic today, the theory of sexual dimorphism is widely accepted as the foundation for any considerations of ammonite phylogeny, ontogeny, taxonomy and even stratigraphy. The concept first appeared in the 19th century (e.g., de Blainville 1840; Munier-Chalmas 1892) and was intended to explain the common occurrence of two more or less similar ammonite morphs which differed in their final size. The breakthrough of the theory was factually in 1962–1963 when Henryk Makowski and John H. Callomon, almost

simultaneously and independently from each other, published their seminal works (Makowski 1962; Callomon 1963) about the sexual dimorphism in Jurassic ammonites, and the concept was immediately applied to Jurassic–Cretaceous ammonite faunas (e.g., Westermann 1964; Lehmann 1966; Kennedy and Cobban 1976; Matyja 1986; Kennedy 1989; Cobban and Kennedy 1993; Maeda 1993).

The phenomenon of sexual dimorphism is probably also represented in many Cretaceous ammonites but very rarely rigorously tested by statistics. Apparently, a sexual dimorphic correspondence is also reflected in three early Turonian ammonite species from the Brießnitz Formation of Saxony, i.e., *Mammites nodosoides* (Schlüter, 1871), *Lewesiceras peramplum* (Mantell, 1822), and *Spathites* (*Jeanrogericeras*) *reveliereanus* (Courtiller, 1860), in which different morphs were visually detected at a glance. However, to rigorously test the hypothesis of a sexual dimorphism and, therefore, to elucidate if there really were reproducible differences among these ammonite faunas and if one can differentiate in fact micro- and macroconchs or not, two complex analytical functions of the computer program PAST 4 were used. The three species from the Brießnitz Formation were selected because they are commonly fairly well preserved and are represented by statistically significant populations.

Institutional abbreviations.—MMG: SaK, Museum für Mineralogie und Geologie Dresden, Senckenberg Naturhistorische Sammlungen Dresden (collection part Saxonian Cretaceous), Germany.

Other abbreviations.—D, maximum diameter; d, larger radius of the shell; e, smaller radius of the shell; T, number of tuberculate bullae (numbers in parentheses of T are the average values); UD, diameter of the umbilicus (numbers in parentheses of UD are dimensions as a percentage of diameter with UD ≤10% = very involute, UD 11–20% = involute, UD 21–30% = moderately involute, UD 31–40% = moderately evolute, UD 41–50% = evolute, and UD ≥50% = very evolute); Wb, whorl breadth of the final whorl; Wh, height of the final whorl; Wb/Wh, ratio of whorl breadth and whorl height (see Fig. 2). LDA, linear discriminant analysis; PCA, principal component analysis.

Geological setting

Cretaceous strata are exposed in Saxony along the course of the Elbe River from the Saxonian Switzerland (Elbsandsteingebirge) in the southeast to Meißen in the northwest, forming the Elbtal Group (Voigt and Tröger in Niebuhr et al. 2007). The Turonian succession was deposited in a seaway between the Mid-European Island to the southwest and the subordinate West-Sudetic Island to the northeast (Fig. 1A, B). Towards the northwest, the Saxonian Cretaceous Basin (SCB) opened into the wide northern German shelf sea while, to the southeast, the Bohemian Cretaceous Basin formed a gateway into the Tethys Ocean (Wiese et al. 2004; Wilmsen and Niebuhr 2014).

The Elbtal Group has a stratigraphic range from the lower Cenomanian into the middle Coniacian (Voigt and Tröger in Niebuhr et al. 2007; Wilmsen and Niebuhr 2014; Niebuhr et al. 2020). Marly-calcareous offshore sedimentation of the Meißen-Dresden Subgroup prevailed in the north-western part of the Saxonian Cretaceous Basin (Wilmsen et al. 2019; Fig. 1C) whereas in the Saxonian Switzerland, siliciclastic shallow-water-sedimentation prevailed (Niebuhr et al. 2020). In the aftermath of the stepwise Cenomanian sealevel rise that caused a time-transgressive onlap of sedimentary strata onto an inherited palaeotopography (Fig. 1C; see Niebuhr and Wilmsen 2023 for a current revision of the Cenomanian in Saxony), two major transgressive pulses in the latest Cenomanian and earliest Turonian resulted in the development of a grain-size graded shelf: offshore deposition prevailed in the Meißen-Dresden area (marls and Pläner deposits of the Brießnitz Formation), grading towards the southeast (Saxonian Switzerland) into shallow-marine siliciclastic strata of the Schmilka Formation (e.g., Beeger 1963; Voigt 1999; Janetschke and Wilmsen 2014).

The Brießnitz Formation, an irregularly stratified, fine-grained, marly-calcareous lithostratigraphic unit of blue- to brown-grey color, ranges chronostratigraphically from the lowermost lower Turonian into the lowermost middle Turonian (Tröger 1988; Tröger and Voigt in Niebuhr et al. 2007). A conspicuous argillaceous interval in its lowermost part, the Lohmgrund Horizon, forms an easily recognizable, fine-grained stratum across different formations (Niebuhr et al. 2020). Up-section, it grades into the Labiatus Pläner (named after the characteristic lower Turonian index inoceramid bivalve *Mytiloides labiatus*), a strongly bioturbated, silty-calcareous sedimentary rock. The Brießnitz Formation has the largest exposure of all the Cretaceous units of the Dresden area and was quarried in numerous places for construction purposes (Beck and Hazard 1892, 1893). It is very fossiliferous, especially with respect to its cephalopod faunas (Tröger 1988; Wilmsen and Nagm 2013, 2014; Wilmsen 2016; Wondrejz 2021; Wilmsen et al. 2021). The ammonite faunas discussed herein have been collected from the lower Turonian Labiatus Pläner of the Brießnitz Formation, formerly widely exposed in eight now abandoned quarries and marl pits in Dresden (=DD)-Brießnitz (abbreviation: Br), DD-Cotta (Co), DD-Gorbis (Go), DD-Kauscha (Kau), DD-Leubnitz (Lb), DD-Leutewitz (Le), DD-Lockwitz (Lo) and DD-Omsewitz (Om) (for locality details, see Wondrejz 2021). Based on the occurrence of the index ammonite *Mammites nodosoides*, the studied faunas can be assigned to the upper part of the lower Turonian (Wright and Kennedy 1981).

Material and methods

In total, 338 specimens comprising three ammonite species have been systematically studied, mostly moderately well
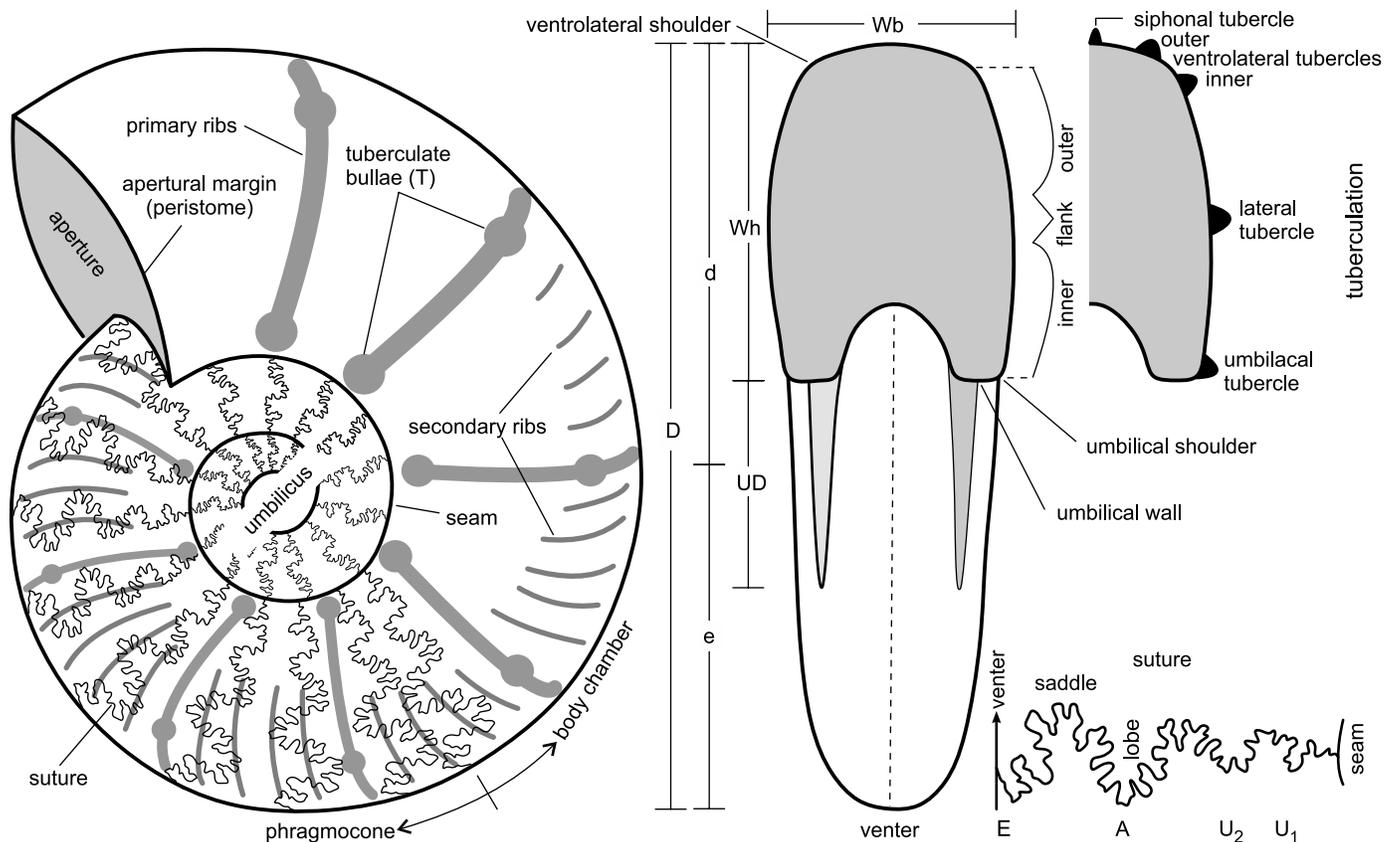
Fig. 2. Ammonite morphological terms and key parameters. Modified after Wilmsen and Nagm (2014). Abbreviations: D, maximum diameter; d, larger radius of the shell; e, smaller radius of the shell; UD, diameter of the umbilicus; Wb, whorl breadth of the final whorl; Wh, height of the final whorl; for the suture line: A, adventive lobe; E, external lobe; U, umbilical lobe.

to incompletely preserved (composite) internal moulds. Due to imperfect preservation, only between 61% and 76% of the studied specimens could be included in the statistical evaluation. The specimens are specifically distributed as follows (total number/statistically treated specimens/percentage):

Lewesiceras peramplum (Mantell, 1822): 83/63/76%;
Mammites nodosoides (Schlüter, 1871): 194/119/61%;
Spathites (*Jeanrogericeras*) *reveliereanus* (Courtiller, 1860): 61/38/62%.

A Vernier Caliper has been used to measure all linear dimensions (given in millimeters) and several parameters were measured and/or calculated, respectively (see Fig. 2 and SOM, Supplementary Online Material available at http://app.pan.pl/SOM/app68-Wondrejz_etal_SOM.pdf, as well as Other abbreviations section above). Morphological terminology follows Arkell (1957). Synonymy lists have been kept short, containing only the first valid introduction of the taxa and important revisions as well as recent records and those of regional palaeontological interest.

For statistical analyses, we used the programme PAST 4 (Hammer et al. 2001; https://www.nhm.uio.no/english/research/resources/past/). The first method utilised in PAST 4 was the classical clustering function. This analytical tool is an explorative procedure to detect similarity structures within datasets. Objects, in our case specimens, can be combined into clusters based on their characteristics. For that matter, each cluster should be homogeneous among itself as much as possible and at the same time different as much as possible (heterogeneous) to the other clusters (Johnson 1967; Kirenz 2020). The arrangement of the objects into the clusters is calculated following specific rules. This decision is not only dependent on the choice of the clustering algorithm (in this case the Ward's method) but also on how the distance/similarity between the clusters is determined (Johnson 1967). One possibility to calculate this similarity is the Euclidean distance, which is the distance between two points, calculated as straight line in the space (linear distance). An Euclidean distance of zero therefore means that the points/objects are identical. The formula for the calculation of the Euclidean distance for n different variables is:

$$d(A,B) = \sqrt{\sum_{i=1}^{n} (A_i - B_i)^2}$$

As clustering algorithm, the Ward's method is a favored variance-based method and was also used in this case. This function combines the clusters that have the smallest growth of the total variance and is therefore an expansion of the empirical variance of one variable for the multivariate use

(Johnson 1967; Kirenz 2020). With the help of a dendrogram, the result of a clustering algorithm can be visualised. The dendrogram should be read from the top to the bottom and describes the process of the clustering in this direction. The vertical axis characterises the heterogeneity of the clusters with the "Cophenetic distance", the smallest distance between two clusters. At the head of the diagram, all specimens are listed separately. Initially, each specimen corresponds therefore to one single cluster, which is shown by an own horizontal line for each specimen. The clusters are then combined gradually from the top to the bottom, which is indicated by the vertical lines between them. The smallest distance between two clusters is at the beginning (top) zero, when each specimen represents its own cluster. Afterwards, the distance is growing monotonously, because more dissimilar clusters with greater distance between each other are combined. At the last junction of all clusters, in one big joint cluster, the distance reaches the maximum value (Kirenz 2020). For application of the Ward's method, it is necessary that no data are missing from any specimen. Therefore, only those specimens could be used for the analysis that more-or-less yielded all measurements. With the classical clustering mode, it was possible to construct a cluster of all tested ammonites to find out which of them form groups and at which point and through which parameter the groups developed morphologically apart.

There are two major analytical methods for a classification of data: principal component analysis (PCA) and linear discriminant analysis (LDA). These techniques are used because of their advantages in data aggregation and dimensionality reduction (Balakrishnama and Ganapathiraju 1998). The difference between the two is that while PCA accounts for the most variance in the whole dataset, the LDA gives the axes that account for the most variance between the individual classes (Raschka 2014). A benefit of linear discriminant analysis is the case where the within-class frequencies are unequal, and their performances have been examined on randomly generated test data. The LDA maximises the ratio of between-class variance to the within-class variance in any particular data set, thereby guaranteeing maximum separability (Balakrishnama and Ganapathiraju 1998).

On the basis of the clusters from the classical clustering, groups of the ammonites could be differentiated and illustrated through the discriminant analysis (LDA) in a graph which shows scatter plots of the groups. For the discriminant analysis, the program needs a classification of the groups. After that, it compares all data of the variables with each other and shows the linear border of each group. For a meaningful computing of the data by the program, it is important that all calculated parameters are grouped in classes. To achieve this, the range between the maximum and the minimum value of one parameter of all ammonites was subdivided in steps to get 4 to 13 classes. The classes of the parameters that have been used herein and the classification are shown in the SOM.

Results and systematic palaeontology

Due to the supposed pairwise occurrence of three ammonite species from lower Turonian strata of the Brießnitz Formation of Saxony in distinct size classes (potential micro- and macroconchs) and their representation in statistically significant populations, the sexual dimorphic correspondence was rigorously tested in *Lewesiceras peramplum*, *Mammites nodosoides* and *Spathites* (*Jeanrogericeras*) *reveliereanus*. The three taxa are briefly described, illustrated and their biometric data have been evaluated using the classical clustering and the linear discriminant analysis functions of PAST 4 (see SOM).

Suborder Ammonitina Hyatt, 1889
Superfamily Desmoceratoidea Zittel, 1895
Family Pachydiscidae Spath, 1922
Genus *Lewesiceras* Spath, 1939

Type species: *Ammonites peramplus* Mantell, 1822; Turonian of Sussex, southern England, UK; by original designation.

Lewesiceras peramplum (Mantell, 1822)

Figs. 3, 4.

1822 *Ammonites peramplus*; Mantell 1822: 200.
1981 *Lewesiceras peramplum* (Mantell, 1822); Wright and Kennedy 1981: 29, pl. 2: 1–3; pl. 3; text-figs. 9, 12. [with synonymy]
2013 *Lewesiceras peramplum* (Mantell, 1822); Wilmsen and Nagm 2013: 650, figs. 3–5.
2014 *Lewesiceras peramplum* (Mantell, 1822); Wilmsen and Nagm 2014: 204, fig. 3a, b.
2014 *Lewesiceras peramplum* (Mantell, 1822); Amédro and Delvaque 2014: 133, pl. 12; pl. 16: 2.
2018 *Lewesiceras peramplum* (Mantell, 1822); Matrion 2018: 192, figs. 128A, 131A.
2019 *Lewesiceras peramplum* (Mantell, 1822); Kennedy and Kaplan 2019: 35, pl. 7: 3, 9, 10, 17; pls. 8–11, 13; text-figs. 15, 16.

Material.—In total, 83 specimens from the lower Turonian (Cretaceous), Brießnitz Formation, Germany, Dresden, locality: Brießnitz (one specimen), Cotta (two specimens), Kauscha (two specimens), Leubnitz (28 specimens), Leutewitz (two specimens), and Lockwitz (48 specimens) were systematically studied. Due to the preservation, only 63 specimens were used for statistical analysis. Repository numbers are provided in SOM 3.

Measurements.—See SOM 3.

Description.—The assemblage consists of large individuals, up to 228 mm in diameter (the average diameter of the Saxonian specimens is 117.5 mm while the largest specimens from the literature measure up to 900 mm), but also small individuals with D ≤60 mm occur. The specimens have a planulate shell at the boundary from moderately involute to moderately evolute (UD ≈30%) with rounded venter. Wb/Wh is approximately 0.58, and the aperture has a high oval to rectangular form. The ornamentation
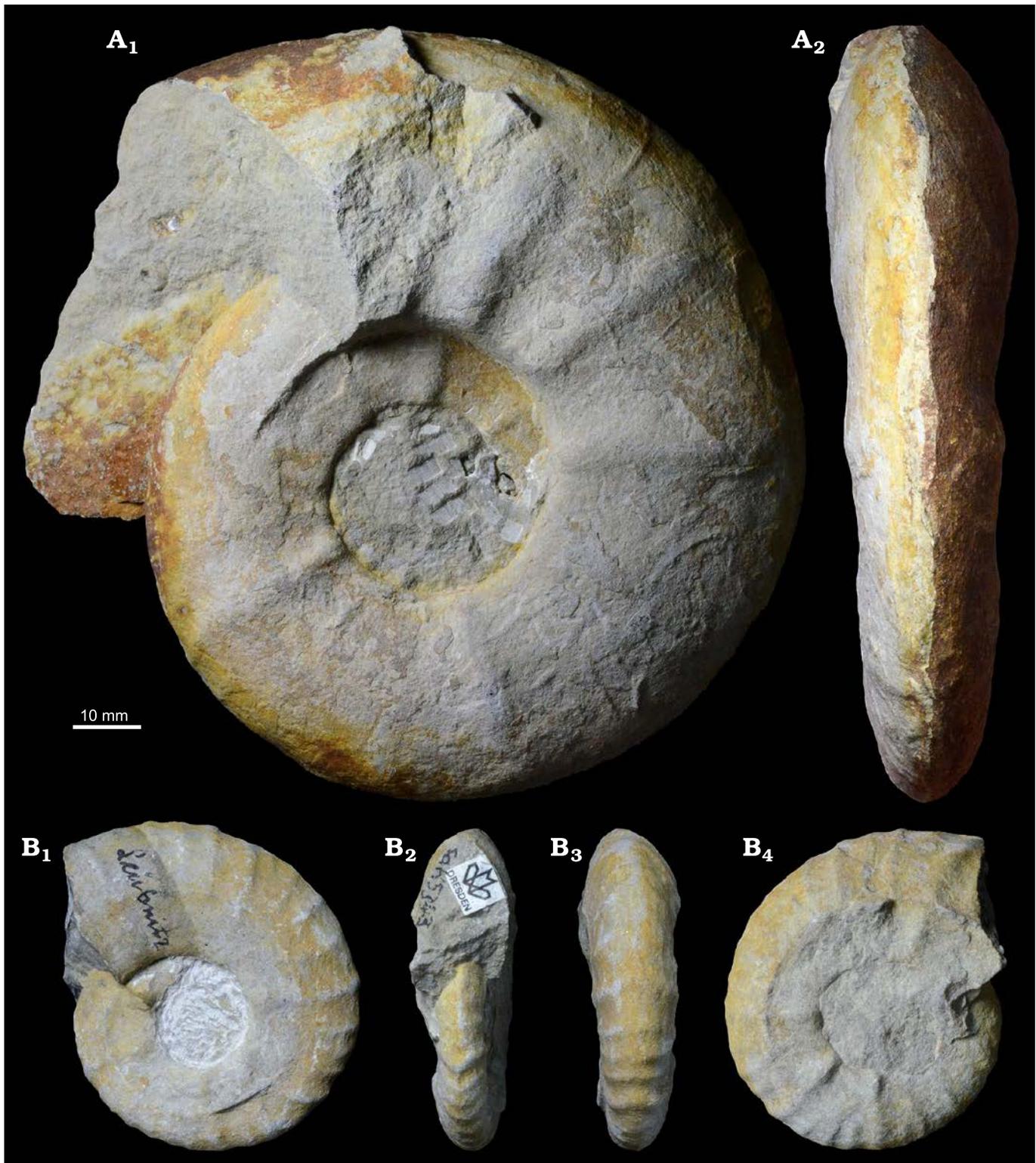
Fig. 3. Photographic illustration of typical large (A) and small (B) specimens of the pachydiscid ammonoid *Lewesiceras peramplum* (Mantell, 1822) from the lower Turonian of the Brießnitz Formation, Dresden, Germany. **A**. MMG: SaK 5163 from Leubnitz, in lateral (A_1) and ventral (A_2) views. **B**. MMG: SaK 5343 from Leutewitz, in lateral (B_1, B_4), apertural (B_2), and ventral (B_3) views.

with the tubercles and ribbing changes during ontogeny, declines at maturity and may disappear completely. The inner whorls are characterised by five to six slightly projecting umbilical tubercles per whorl, giving rise to rather narrow, irregular, and curved primary ribs and two to four short secondary ribs. Later, the umbilical tubercles become weaker and bullate, the primary ribs become lower, and the secondary ribs increase in number and weaken. At a di-
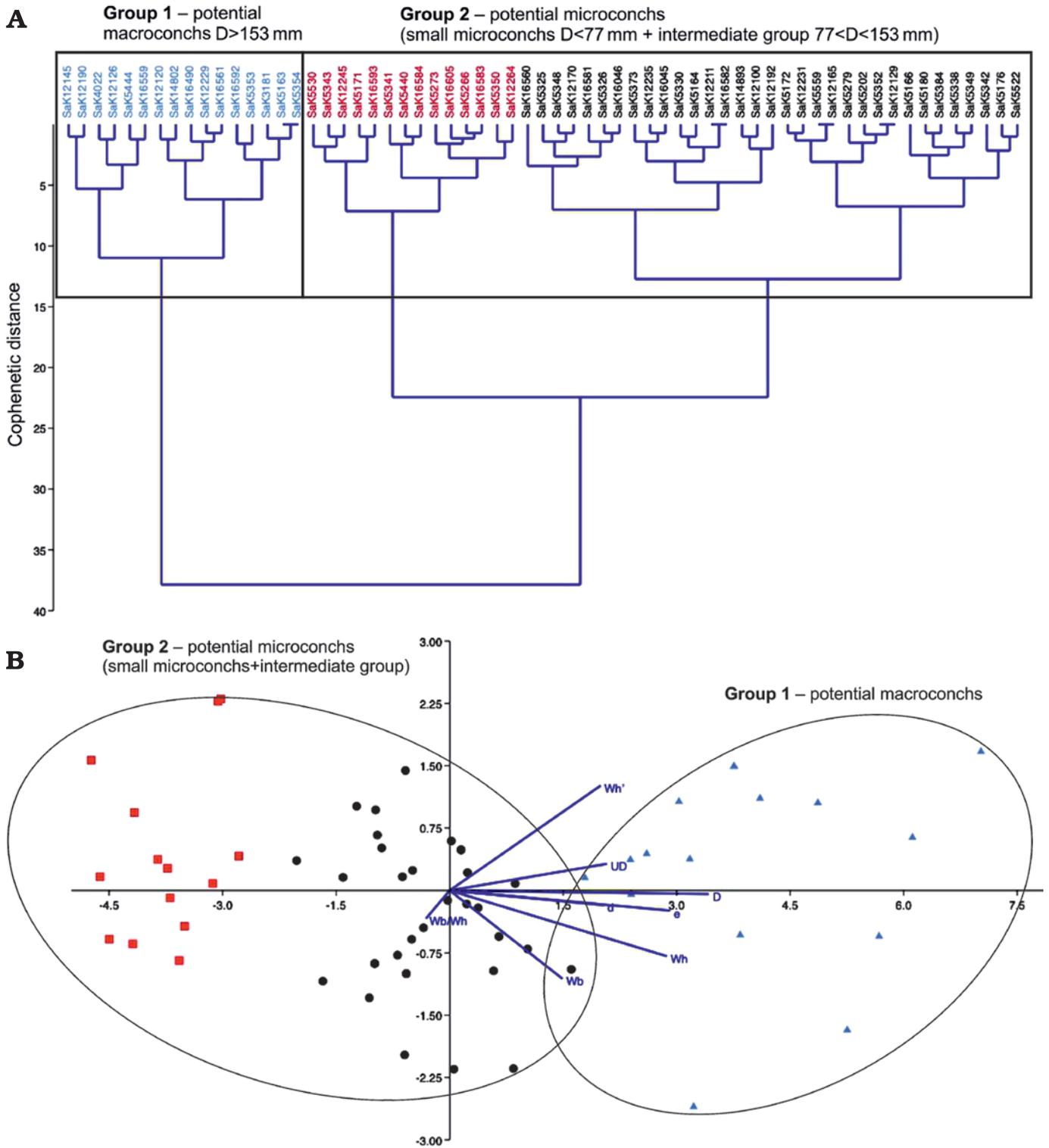
Fig. 4. Statistical test of potential dimorphism in *Lewesiceras peramplum* (Mantell, 1822) based on 63 specimens. The repository number of each speci-men is given on top of the diagram. **A**. Classical clustering; the red color characterises particularly small individuals with D <77 mm in between the group of potential microconchs. **B**. Linear discriminant analysis (LDA); the color code follows the assignment of the classical clustering above. The dark blue lines are biplots of all variables, an overlaying of a score plot and a loadings plot in a single graph, which enables to visualise high-dimensional data by using a two-dimensional graph.

ameter of approximately 100 mm, the secondary ribs have normally disappeared, and the primary ribs are weak or absent on the venter. All ribs are separated from each other through intercostal sections, which have the same width as the ribs. The umbilicus is shallow to moderately deep, and the umbilical border is rounded.

Stratigraphic and geographic range.—*Lewesiceras peramplum* occurs abundantly in the lower and middle Turonian of Germany, the Czech Republic, Poland, France, Tunisia, and Morocco (Wright and Kennedy 1981). Wilmsen and Nagm (2013) suggested that the species may have originated already in the latest Cenomanian and may range into the early late Turonian based on records from Saxony.

Statistical analyses.—Classical clustering and linear discriminant analysis, considering eight morphological variables, were executed for all 63 relevant specimens (see Fig. 4 and SOM). In the classical clustering diagram, two large groups (inferred micro- and macroconchs) emerged, which differ primarily in the maximum diameter, similarly to the situation in *M. nodosoides* (see below). The Cophenetic distance at the last joint cluster (bottom of the diagram) is 38, and therefore the two large groups are more similar than those of *M. nodosoides*, probably due to the lower sample number. The LDA of *L. peramlum* shows again two large groups, which are broadly distributed but also in total farther away from each other. Nevertheless, they slightly overlap in the lower part of the diagram.

Superfamily Acanthoceratoidea de Grossouvre, 1894

Family Acanthoceratidae de Grossouvre, 1894

Subfamily Mammitinae Hyatt, 1900

Genus *Mammites* Laube and Bruder, 1887

Type species: *Ammonites nodosoides* Schlüter, 1871; lower Turonian of Westphalia, northern Germany; by monotypy.

Mammites nodosoides (Schlüter, 1871)

Figs. 5, 6.

1871 *Ammonites nodosoides*; Schlüter 1871: 19, pl. 8: 1–4.
1981 *Mammites nodosoides* (Schlüter, 1871); Wright and Kennedy 1981: 75, pl. 17: 3; pl. 19: 3; pl. 20: 4; pl. 22: 4; pl. 23: 1–3; pl. 24: 2, 3; text-figs. 19B, 23, 24. [with full synonymy].
2013 *Mammites nodosoides* (Schlüter, 1871); Wilmsen and Nagm 2013: 666, figs. 17G, H, 18A, B.
2014 *Mammites nodosoides* (Schlüter, 1871); Wilmsen and Nagm 2014: 218, fig. 10a, b.
2014 *Mammites nodosoides* (Schlüter, 1871); Amédro and Delvaque 2014: 144, pl. 3: 1, 2.
2016 *Mammites nodosoides* (Schlüter, 1871); Kennedy and Gale 2016: 278, fig. 18.
2018 *Mammites nodosoides* (Schlüter, 1871); Matrion 2018: 195, fig. 129A, B.
2019 *Mammites nodosoides* (Schlüter, 1871); Kennedy and Kaplan 2019: 49, pls. 19–21.

Material.—In total, 194 specimens from the lower Turonian (Cretaceous), Brießnitz Formation, Germany, Dresden, locality: Leubnitz (81 specimens), Leutewitz (three specimens), Lockwitz (107 specimens), and Omsewitz (three specimens), were systematically studied. Due to preservational issues, only 119 specimens could be used for statistical analyses. Repository numbers are provided in SOM 4.

Measurements.—See SOM 4.

Description.—This large species is very abundant in Saxony; the largest specimen reaches a diameter of 384 mm, but there are also many small individuals with D <50 mm. With a UD of 26.3%, *M. nodosoides* is moderately involute. The Wb/Wh ratio is 0.8 on average, which defines a slightly compressed, rectangular whorl cross-section. The umbilicus is moderately deep and has a broadly rounded shoulder and a convex wall. The number of umbilical tubercles ranges from seven to eleven per whorl; they are the source for pairs of weak and broad ribs. Those ribs carry prominent rounded inner- and clavate outer ventrolateral tubercles. During ontogeny, the inner ventrolateral tubercles migrate up the venter and merge with the outer ventrolateral ones. The umbilical tubercles bloat during ontogenetic growth. The result of this development is that adult individuals of *M. nodosoides* show large umbilical and ventrolateral horns. The venter is flat to slightly concave, and the flanks are flat and parallel.

Stratigraphic and geographic range.—*Mammites nodosoides* is the index ammonite of the eponymous upper lower Turonian standard ammonite zone and was recorded from several European countries, the Middle East, northern Africa, Madagascar and North as well as South America (Wright and Kennedy 1981).

Statistical analyses.—After the measurement and/or calculation of nine relevant morphological variables, classical clustering and linear discriminant analysis were executed on 119 specimens (see Fig. 6 and SOM). In the classical clustering, two large groups emerged (group 1 and 2). The first group is characterized by large, the second one by medium- and small-sized specimens with respect to maximum diameters. The Cophenetic distance (the smallest distance between two clusters) reaches the high maximum value of 60 at the last junction of all clusters in one big joint cluster. This value might have been caused by the high number of individuals. In the LDA diagram, two scatter plots of the large groups are visible. The values of both groups are broadly distributed; they overlap in the lower part of the diagram.

Genus *Spathites* Kummel and Decker, 1954

Type species: *Spathites chispaensis* Kummel and Decker, 1954; Turonian of Texas, USA and northern Mexico; by original designation.

Subgenus *Spathites* (*Jeanrogericeras*) Wiedmann, 1960

Type species: *Ammonites reveliereanus* Courtiller, 1860; Turonian of the Touraine, France; by original designation of Wiedmann (1960: 741).

Spathites (*Jeanrogericeras*) *reveliereanus* (Courtiller, 1860)

Figs. 7–10.

1860 *Ammonites reveliereanus*; Courtiller 1860: 249, pl. 2: 5–8.
1980 *Spathites* (*Jeanrogericeras*) *reveliereanus* (Courtiller); Kennedy et al. 1980: 826, pls. 105: 1–12; pl. 106: 1–2; text-figs. 3, 5, 6. [with synonymy]
2013 *Spathites* (*Jeanrogericeras*) *reveliereanus* (Courtiller, 1860); Wilmsen and Nagm 2013: 664, figs. 15, 16, 17A–F.
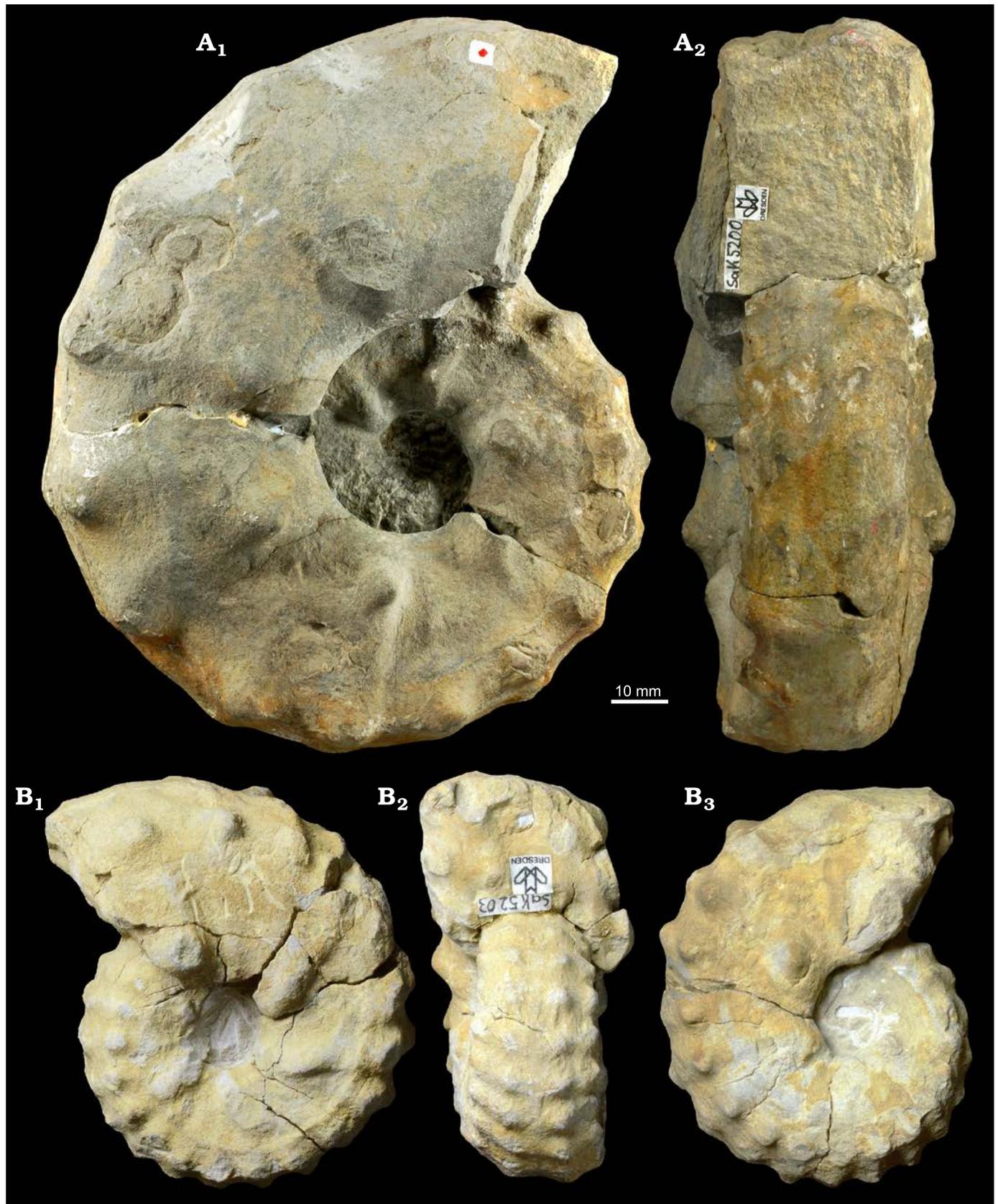
Fig. 5. Photographic illustration of typical large (A) and small (B) specimens of the acanthoceratid ammonoid *Mammites nodosoides* (Schlüter, 1871) from the lower Turonian of the Brießnitz Formation, Leubnitz, Germany. **A**. MMG: SaK 5200 in lateral (A_1) and apertural (A_2) views. **B**. MMG: SaK 5203 in lateral (B_1, B_3) and apertural (B_2) views.
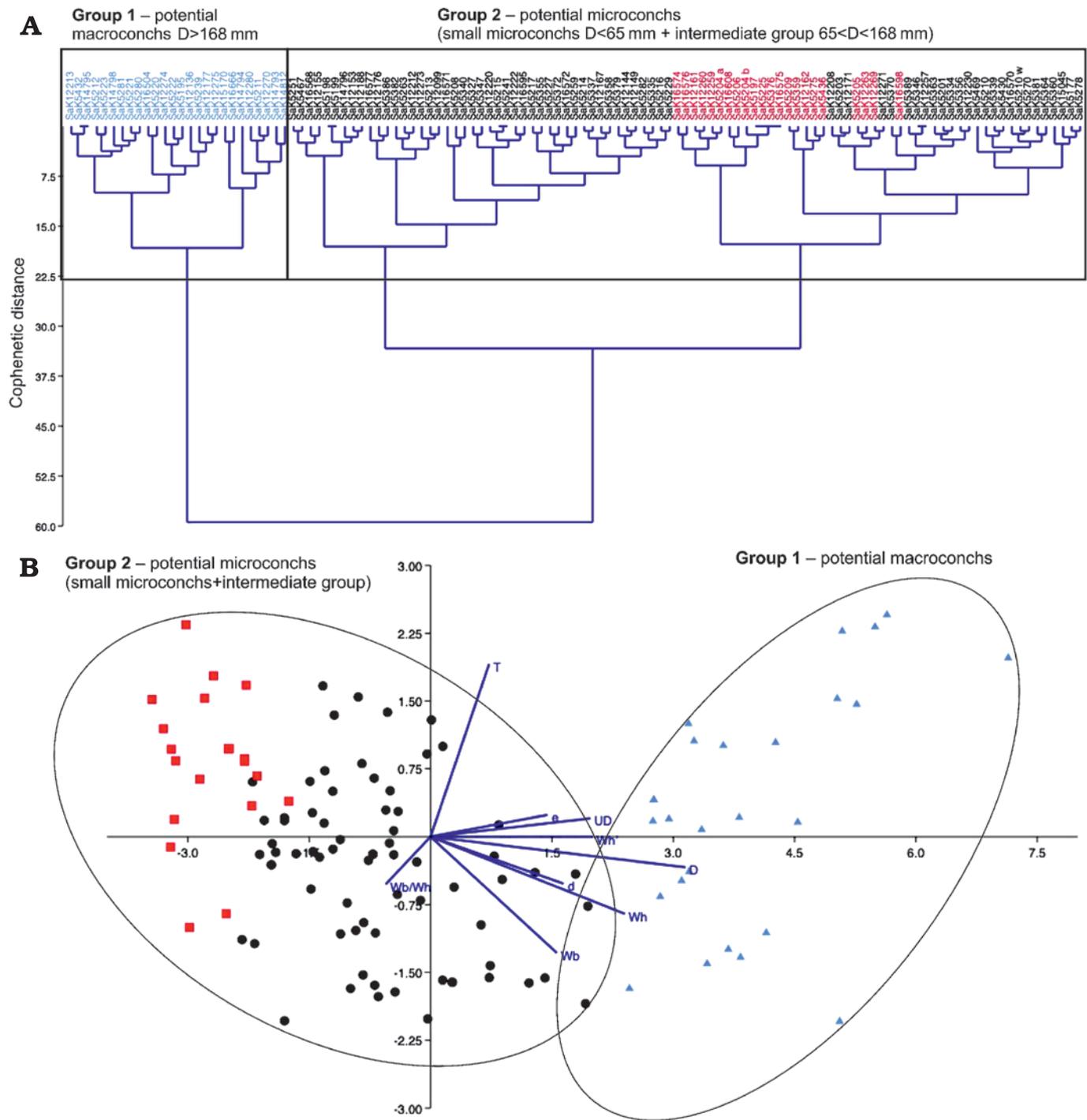
Fig. 6. Statistical test of potential dimorphism in *Mammites nodosoides* (Schlüter, 1871) based on 119 specimens. The repository number of each specimen is given on top of the diagram. **A**. Classical clustering; the red color characterises particularly small individuals with D = 33–65 mm in between the large group of potential microconchs. **B**. Linear discriminant analysis (LDA); the color code follows the assignment of the classical clustering above. The dark blue lines are biplots of all variables, an overlaying of a score plot and a loadings plot in a single graph, which enables to visualise high-dimensional data by using a two-dimensional graph.

2014 *Spathites* (*Jeanrogericeras*) *reveliereanus* (Courtiller, 1860); Wilmsen and Nagm 2014: 216, fig. 9a.

2014 *Spathites* (*Jeanrogericeras*) *reveliereanus* (Courtiller, 1860); Amédro and Delvaque 2014: 143, pl. 13: 2.

2015 *Spathites* (*Jeanrogericeras*) *revelieranus* (Courtiller, 1860); Kennedy et al. 2015: 465, fig. 21A–C.

2016 *Spathites* (*Jeanrogericeras*) *revelerianus* (Courtiller, 1860); Kennedy and Gale 2016: 273, figs. 9–11.

2018 *Spathites* (*Jeanrogericeras*) *reveliereanus* (Courtiller, 1860); Matrion 2018: 195, figs. 132C, D, 136B, 138A, B, 139A, B, 140A.

Material.—In total, an assemblage of 61 specimens from the lower Turonian (Cretaceous), Brießnitz Formation,
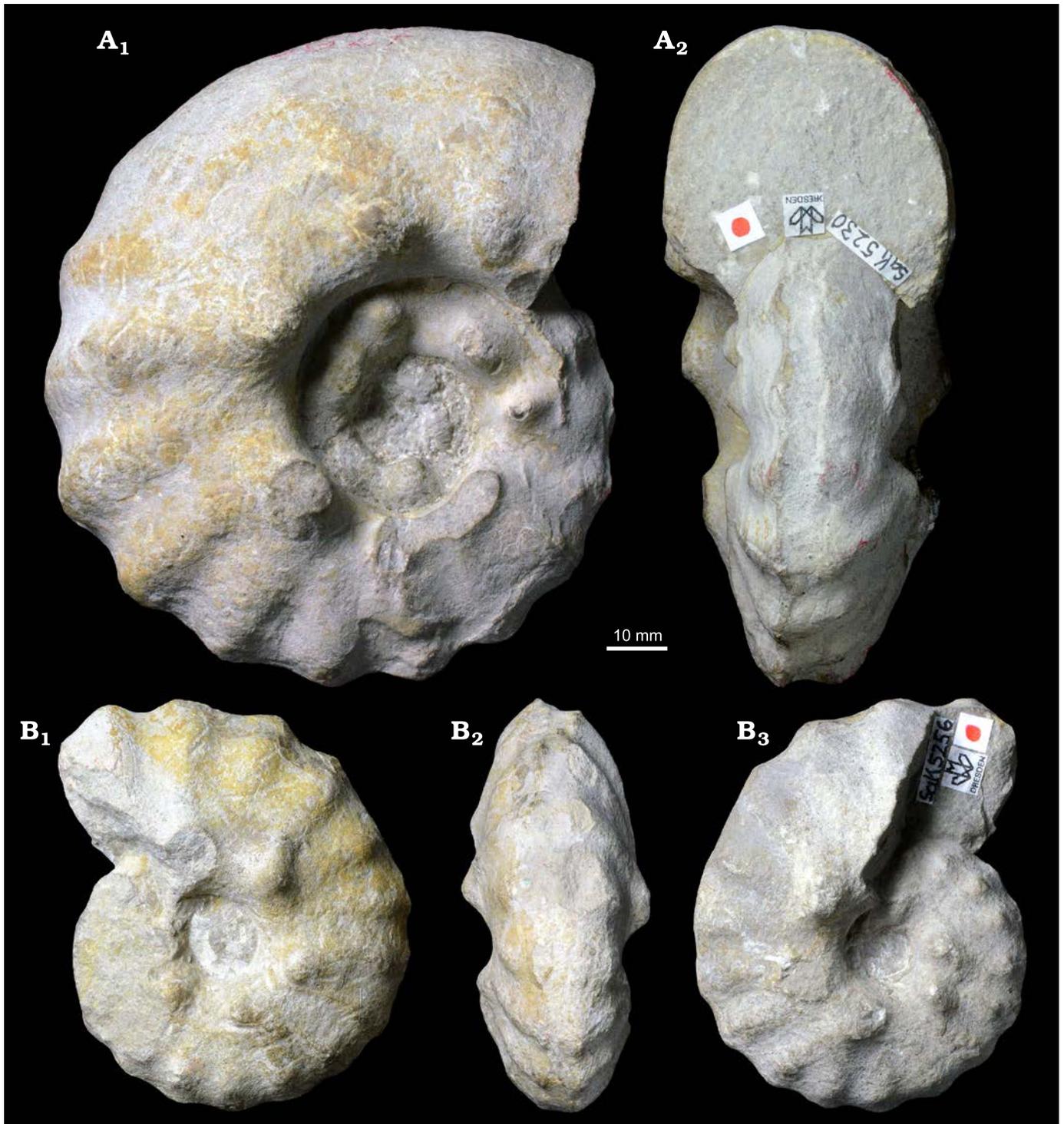
Fig. 7. Photographic illustration of typical large (A) and small (B) specimens of the acanthoceratid ammonoid *Spathites* (*Jeanrogericeras*) *reveliereanus* (Courtiller, 1860) from the lower Turonian of the Brießnitz Formation, Leubnitz, Germany. **A**. MMG: SaK 5230 in lateral (A_1) and apertural (A_2) views. **B**. MMG: SaK 5256 in lateral (B_1, B_3) and ventral (B_2) views.

Germany, Dresden, locality: Leubnitz (35 specimens), Lockwitz (25 specimens), Omsewitz (1 specimen). Due to imperfect preservation, only 38 could be used for the statistical analysis (see SOM). Repository numbers are provided in SOM 5.

Measurements.—See SOM 5.

Description.—Medium-sized to large species, which is moderately involute coiled (UD ≈ 24.7%). There are many relatively large specimens with diameters >100 mm and also many smaller specimens with D ≈ 50 mm. Large specimens have a broader quadrate apertural cross-section with broadly rounded venter, reflecting higher Wb/Wh ratios, while in
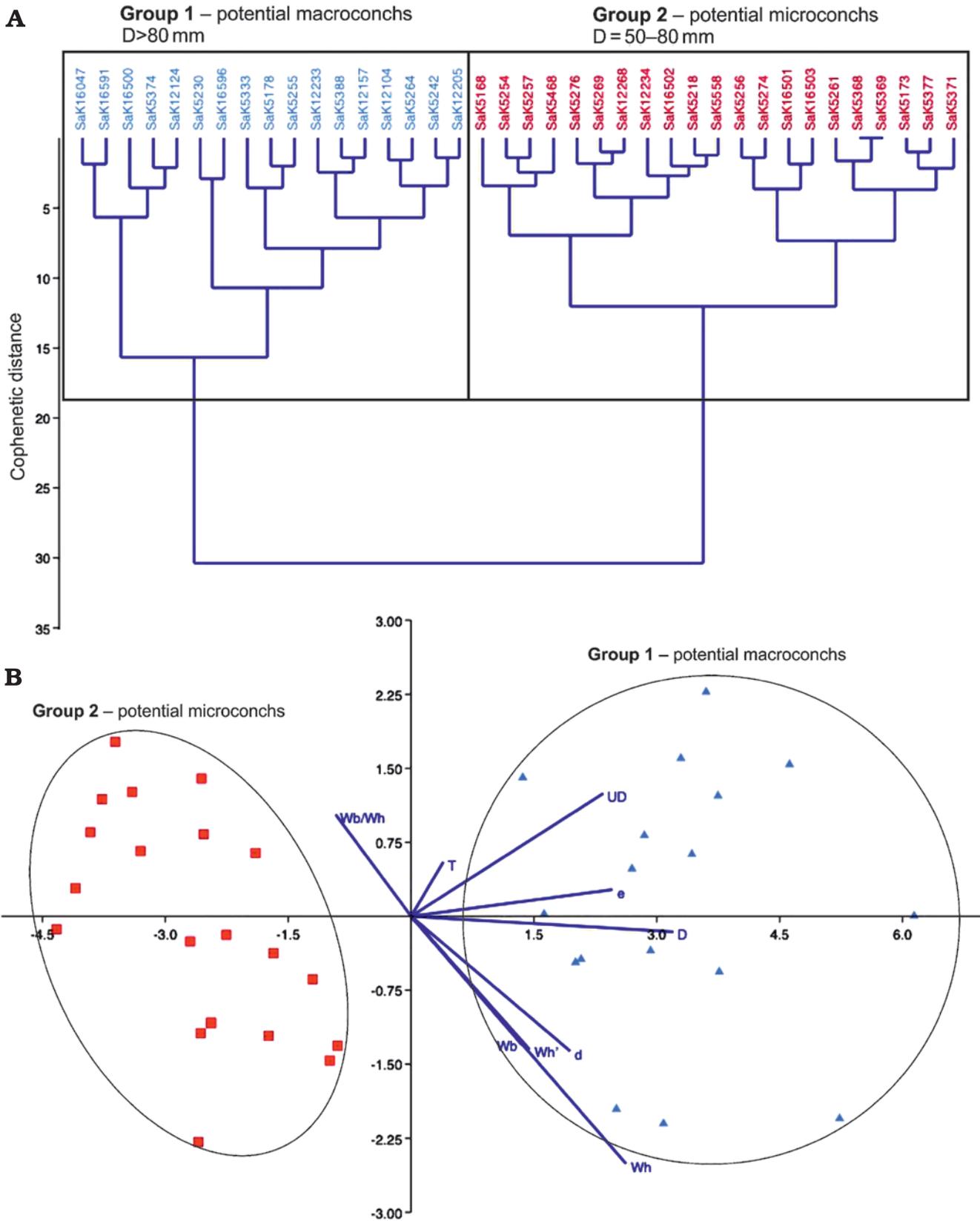
Fig. 8. Statistical test of potential dimorphism in *Spathites* (*Jeanrogericeras*) *reveliereanus* (Courtiller, 1860) based on 38 specimens. The repository number of each specimen is given on top of the diagram. **A**. Classical clustering; inferred macro- and microconchs are marked by blue and red colors, respectively. **B**. Linear discriminant analysis (LDA); the color code follows the assignment of the classical clustering above. The dark blue lines are biplots of all variables, an overlaying of a score plot and a loadings plot in a single graph, which enables to visualise high-dimensional data by using a two-dimensional graph.

smaller individuals, the Wb/Wh ratio is lower, and their cross-section is more rectangular. The flanks are weakly convex in intercostal section. The ventrolateral shoulders are narrowly rounded, and the venter is slightly convex. The strong and straight primary ribs develop in pairs at commonly eight umbilical tubercles per whorl. Approximately at mid-flank, intercalated secondary ribs appear. Each rib carries strong outer ventrolateral bullae. The umbilicus is very deep, the umbilical wall is steep, and the umbilical shoulder is rounded.

Stratigraphic and geographic range.—*Spathites* (*Jeanrogericeras*) *reveliereanus* is known from the lower Turonian *Mammites nodosoides* Zone and the middle Turonian *Collignoniceras woollgari* Zone of Europe (France, Spain, Germany, Romania), India and Morocco (see Wilmsen and Nagm 2013 and Kennedy and Gale 2016 for further details).

Statistical analyses.—Based on the measurement and/or calculation of eight relevant morphological variables, classical clustering and linear discriminant analysis were conducted on the 38 relevant specimens (see Fig. 8 and SOM). In the classical clustering analysis, two groups are clearly separated from each other. The Cophenetic distance is not quite high with 30, but that can be explained by the relatively low number of individuals in comparison to the other two studied species. In the LDA, the two groups are again conspicuously apart from each other and not as scattered as in the other species, i.e., they appear to be more coherent.

Discussion

Dimorphism in ammonites was a long-debated topic among palaeontologists over several decades, sparked by the seminal works about potential sexual dimorphism in Jurassic ammonites published by Makowski (1962) and Callomon (1963). It is now widely agreed that in temporally and spatially concordant populations, macroconch ammonites were the females and the microconchs were the males (e.g., Palframan 1966, 1967; Guex 1970; Lehmann 1981, among many others), because the females might need more space for the gonads and eggs; furthermore, the maturation of the eggs usually takes longer than that of spermatophores, implying a longer lifespan and thus a larger adult size (Lehmann 1981; Vollrath 1998; see also Davis et al. 1996 and Klug et al. 2015c for compilations on dimorphism in ammonoids). However, not all ammonoids show such a dimorphism, and in some cephalopod groups, the males could even be slightly larger than the females, e.g., in the Recent *Nautilus*, the males are slightly larger than the females (Ward 1987; Ward et al. 2016) and in extant coleoids such as *Loligo plei*, males are almost twice as large as females (Hanlon 1982). Furthermore, the large variability in ammonoid size and shape shows that there are large differences in the reproduction strategies between different groups, and these differences may have an impact on the morphology (Ritterbush et al. 2014). Finally, the correspondence of micro- and macroconchs in many inferred dimorphic pairs is based on visual inspection only, has rarely been rigorously statistically tested and often remains largely undocumented, especially with respect to Cretaceous non-scaphitid taxa (see Kennedy 1989). Because of their characteristic uncoiled body chambers, maturity is easily recognized in Scaphitidae and many Cretaceous examples of dimorphic pairs are related to these heteromorph ammonites in which dimorphism is manifested not only by terminal size or modifications of the aperture but also by differences in proportions of the shafts (e.g., Makowski 1962; Cobban 1969; Kennedy 1989; Landman and Waage 1993; Machalski 2005; Landman et al. 2008; Tanabe 2022). However, dimorphism in other Cretaceous ammonite groups is less well documented (Kennedy 1989), but see Maeda (1993) for a careful case study on dimorphism in *Yokoyamaoceras ishikawai*, a Santonian–Campanian representative of the Kossmaticeratidae.

In order to substantiate the conspecifity of two different adult forms (inferred males and females), some key criteria should be fulfilled according to Makowski (1962), Callomon (1963), Palframan (1966, 1967), Davis (1972), Matyja (1986), Davis et al. (1996), and Klug et al. (2015c): (i) the antidimorphs should differ in adult morphology (when different final size is one criterion, these two forms may be called micro- and macroconch, respectively); (ii) they should have more-or-less identical early ontogenies; (iii) antidimorphs should lack of intermediate forms in the adult stage; and (iv) they should have the same stratigraphic ranges and overlapping biogeographic occurrences.

We will discuss these criteria along with the results of our statistical biometric evaluation for the studied ammonite faunas from the Brießnitz Formation below. It should be noted that mature modifications are crucial for the evaluation of dimorphism in order to support the adulthood of the specimens under consideration (e.g., Kennedy 1989; Davis et al. 1996; Klug et al. 2015c; Aiba 2022; Jattiot et al. 2023). However, due to the often imperfect preservation, adulthood is difficult to prove for parts of the studied assemblages due to the absence of unequivocal mature modifications, and this limitation turned out to be a critical point in refusing a dimorphism for two of the three species under investigation. In one species, on the other hand, mature modifications and the emergence of two statistically clearly separated groups of different size support the existence of a dimorphic pair.

***Lewesiceras peramplum* (Mantell, 1822) and *Mammites nodosoides* (Schlüter, 1871).**—The genus *Lewesiceras* is markedly dimorphic according to Wright and Kennedy (1984: 63) and also for *M. nodosoides*, a dimorphism was suspected (Wright and Kennedy 1981: 77, 80; Wilmsen and Nagm 2013: 666). A detailed visual examination of all analysis-relevant representatives of *L. peramplum* (63) and *M. nodosoides* (119) in fact tends to divide the populations into two or three groups. Intuitively, one would classify
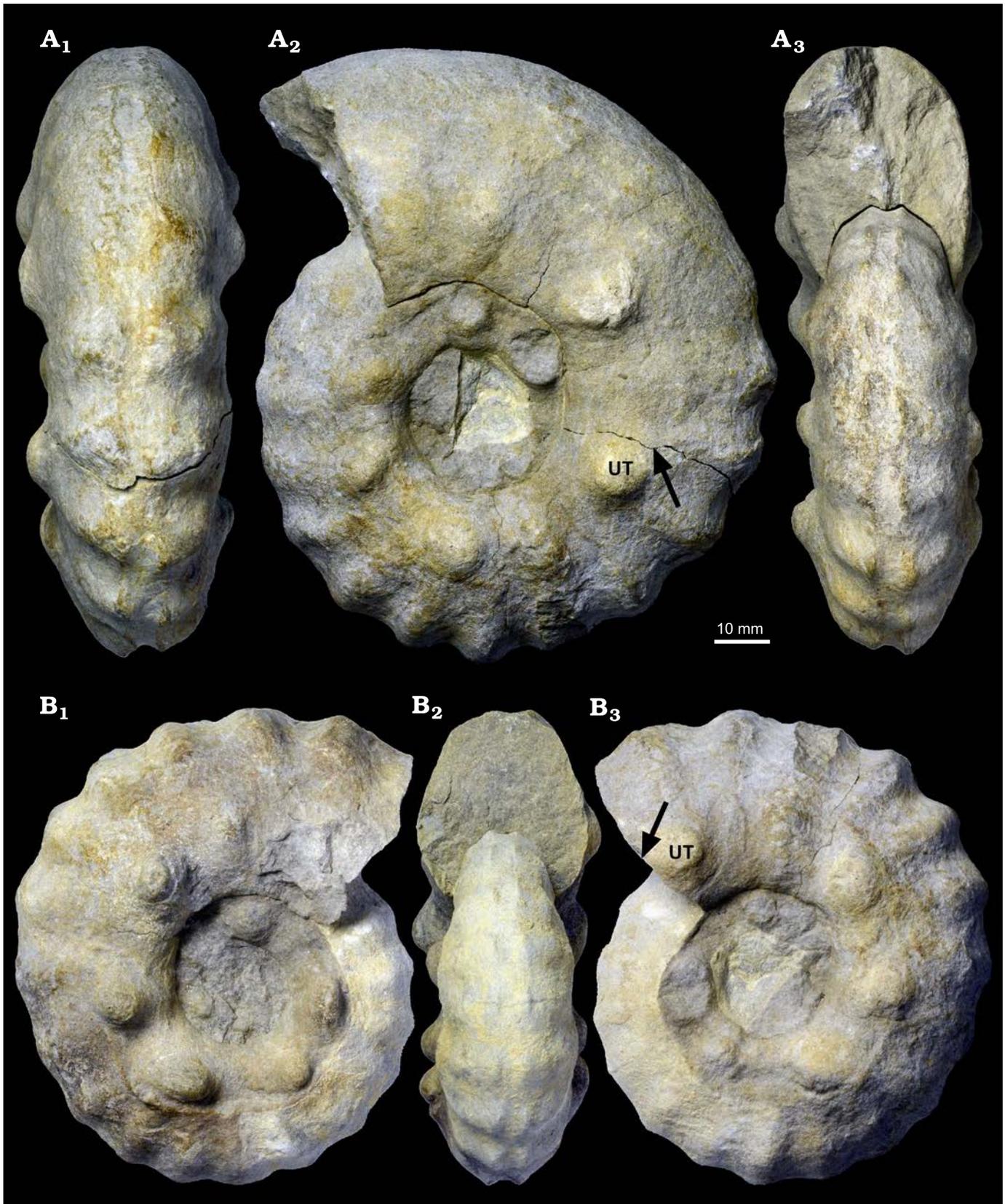
Fig. 9. Acanthoceratid ammonoid *Spathites* (*Jeanrogericeras*) *reveliereanus* (Courtiller, 1860) MMG: SaK 16896 from the lower Turonian of the Brießnitz Formation, Leubnitz, Germany. **A**. Outer whorl in ventral (A₁), lateral (A₂), and apertural (A₃) views; the fracture at which the outer whorl separates from the inner whorl (arrow) and an umbilical tubercle (UT) are marked. **B**. Inner whorl in lateral (B₁, B₃) and apertural (B₂) views; the umbilical tubercle (UT) and the position of the fracture shown in A₂ are marked by arrow.

the very small specimens, such as MMG: SaK 5205 of *M. nodosoides* or MMG: SaK 5273 of *L. peramplum*, as microconchs (group 1) (Figs. 3, 5). The remaining, larger representatives of the two species can be seen either together as a variable group of macroconchs—group 2, or as medium-sized representatives of a transition group (MMG: SaK 5203 of *M. nodosoides*/MMG: SaK 5559 of *L. peramplum*) and large macroconchs (MMG: SaK 16666 of *M. nodosoides* and MMG: SaK 5163 of *L. peramplum*), groups 2 and 3, respectively. Only the first alternative of classification with two groups, micro- and macroconchs, would directly reinforce a possible sexual dimorphism, since only two sexes can be distinguished (two groups), and one of the diagnostic features for sexual dimorphisms in ammonites is the lack of intermediate forms in the adult stage (Makowski 1962; Matyja 1986). However, as pointed out by Kennedy (1989), ammonites in which characters other than final size define a dimorphism may well show an overlap of micro- and macroconch size. With respect to similar early ontogenies it can only be stated that the morphology of the small specimens commonly fully corresponds to the morphology of the inner whorls of larger specimens as can be seen when the whorls of the latter came apart.

Since purely visual classifications do not represent a significant proof of an existing or non-existing sexual dimorphism, and, to make matters worse, no reliable traits of adulthood such as apertural modifications or septal crowding (cf. Davis et al. 1996; Klug et al. 2015c) can be recognised in our populations due to imperfect preservation, two statistical analyses were carried out for each species using PAST 4. Eight or nine morphometric variables were measured and/or calculated for each ammonite (see methodology chapter and SOM), and these values were afterwards evaluated using two multivariate methods, i.e., classic clustering and the linear discriminant analysis (LDA).

The results of the clustering analysis of *M. nodosoides* are, as shown in Fig. 6, two large groups, i.e., a well-defined first group of macroconchs with a D >168 mm and a very diverse second group of potential microconchs with D = 33–168 mm. For the purpose of visual illustration, very small representatives (D = 33–65 mm) discriminated purely visually were colored in red to show their position within the second group (Fig. 6). They cannot be clearly assigned to any cluster but are distributed within the large group 2.

A similar cluster diagram emerged for *L. peramplum* (see Fig. 4). Here, the large inferred macroconchs with a D >153 mm (group 1) are clearly delineated, while small- and medium-sized representatives form a variable second group of potential microconchs (D <153 mm). For *L. peramplum*, however, the very small representatives are clearly delimited (colored in red in Fig. 4) within the large group 2 of inferred microconchs (compared to *M. nodosoides*), forming a distinct subgroup.

The linear discriminant analysis confirms the classification of the clusters for *M. nodosoides* and *L. peramplum*. In the right area of the diagrams (Figs. 4, 6), where larger maximum diameters are plotted, the large macroconchs are situated (shown in blue). Further to the left, all other ammonites are shown, scattered as group two in a relatively wide area. Although the scatter plots of the potential macro- and microconchs are classified as independent large groups in the cluster analysis, they are not far apart in the discriminant analysis and even overlap partially (see Figs. 4, 6). Therefore, in the cases of *M. nodosoides* and *L. peramplum*, the cluster and discriminant analyses are not clearly expedient in order to independently confirm or reject a dimorphism.

All the specimens studied herein were not ideally preserved, which means that characteristics such as the number of umbilical or ventrolateral tubercles and ribs could not be recorded for all of the representatives. In *M. nodosoides*, the umbilical tubercles were recorded in most of the representatives, and with the others the average value of the number of umbilical tubercles of the recorded individuals was used, since PAST 4 cannot work with "non-information". In *L. peramplum* in particular, it was only possible to work with eight variables, as the ribbing was only visible in some specimens. However, since the tubercles and ribs could be a decisive factor for the classification of sexual dimorphisms, it can be concluded that the statistical analyses of both *L. peramplum* and *M. nodosoides* do not provide any significant certainty regarding the presence or absence of a sexual dimorphism.

Unfortunately, the exact stratigraphic horizons from which the specimens derive are unknown. Thus, an evaluation of possible temporal trends is impossible, and the specific groups must be regarded as single late early Turonian assemblages. Based on an estimated duration of ca. 800 kyr for the early Turonian (e.g., Richardt et al. 2013; Laurin et al. 2021), and the observation that the studied ammonite faunas do not represent the commonly poorly fossiliferous lowermost Turonian succession in Saxony, we conclude for about 500 kyr of geological time, corresponding to the late early Turonian *M. nodosoides* Zone (ca. 93.5–93.0 Ma in the Geological Timescale 2020; Gale et al. 2020). The spatial distribution of both species shows that the specimens of the two taxa are not from one locality but were instead found scattered across eight different former pits. However, the depositional environment of the Brießnitz Formation was relatively uniform across the studied area as can be demonstrated by the monotonous fine-grained lithofacies, and habitat differences can thus largely be excluded as a driver of morphological disparity. Furthermore, the study area is relatively small (less than 100 km^2). In a nutshell, within the limitations of the above mentioned stratigraphic resolution, we may conclude that the studied fossil assemblages in fact had the same stratigraphic ranges and overlapping biogeographic occurrences (cf. Davis et al. 1996; Klug et al. 2015c).

On the other hand, apart from maximum diameter, no further features can be recognised in both *M. nodosoides* and *L. peramplum* that differ significantly between the groups. Due to the absence of ontogeny-specific characteristics, such as a differentiation of the aperture or sutural approximation,

it cannot be assumed that all studied specimens have been preserved in full size. It is more likely that smaller representatives are just incompletely preserved and are therefore only inner whorls of originally larger ammonites (in fact, the small specimen of *M. nodosoides* shown in Fig. 5B, MMG: SaK 5203, is fully septate and thus, demonstrably incompletely preserved). This interpretation may find further support in the facts that *L. peramplum* can reach maximum sizes of up to 900 mm (Wright and Kennedy 1981) while our largest specimen has only a diameter of 228 mm, and that (potentially incompletely preserved) small forms dominate the assemblages. In a nutshell, if preservation is included in the evaluation, neither in *M. nodosoides* nor in *L. peramplum* from the lower Turonian strata of the Brießnitz Formation, a sexual dimorphism can be proven. Rather, a combination of large intraspecific variability and differential preservation that often led to incompletely preserved specimens dissembles dimorphic populations at a first glance.

Spathites (*Jeanrogericeras*) *reveliereanus* (Courtiller, 1860).

—In comparison to *M. nodosoides* and *L. peramplum*, the 38 moderately to well preserved (= relevant) specimens of *Spathites* (*Jeanrogericeras*) *reveliereanus* from the lower Turonian of the Brießnitz Formation showed a much clearer pattern with respect to a potential sexual dimorphism.

Already through an initial visual inspection, differences between the large macroconchs (group 1) and smaller microconchs (group 2) could readily be observed (Fig. 7). Obviously, the specimens have a significant different maximum diameter and, due to proportionality, also UD, but in addition to that there is a distinct difference of the aper-

tural cross-section between those two groups. Specimens of the first group (e.g., MMG: SAK 5230) have a broader, quadrate apertural cross-section with broadly rounded, non-sulcate venter reflecting higher Wb/Wh ratios, while in individuals of the second group, such as MMG: SAK 5256, the Wb/Wh ratio is smaller, their cross-section is more high-rectangular and the venter remains sulcate throughout ontogeny (Fig. 7).

These findings also appear in the analysis with PAST 4. The classical clustering separates the specimens of *S.* (*J.*) *reveliereanus* precisely into the previously expected two groups (see Fig. 8A). The macroconchs (blue) have a maximum diameter >80 mm, while the microconchs (red) range between 50 and 80 mm. This classification is confirmed by the discriminant analysis (Fig. 8B), where two clearly separated scatter plots emerge, on the left-hand side, the microconchs with small diameters and on the right-hand side, the macroconchs with larger values of D. There are no intermediate forms and both groups are almost equally large (21 microconchs versus 17 macroconchs).

For the stratigraphic occurrence of the investigated specimens of *S.* (*J.*) *reveliereanus* from the Brießnitz Formation of the Dresden area, the same limitations apply as discussed above for *M. nodosoides* and *L. peramplum*. However, within the restricted biostratigraphically constrained interval of geological time (≤500 kyr) the fauna can be regarded as an almost contemporaneous fossil assemblage from a palaeobiogeographic entity. Again, the early ontogeny seems to be identical as can be judged from occasionally visible inner whorls of larger specimens as the widening and ventral rounding of the body chamber occurs beyond a diameter of

[M]
− D_{max} >80–152 mm
− rounded, inflated adult body chamber
− adult venter non-sulcate
− effacing ornament on adult body chamber

[m]
− D_{max} ≤80 mm
− compressed body chamber
− adult venter sulcate
− strong ornament persisting in adulthood
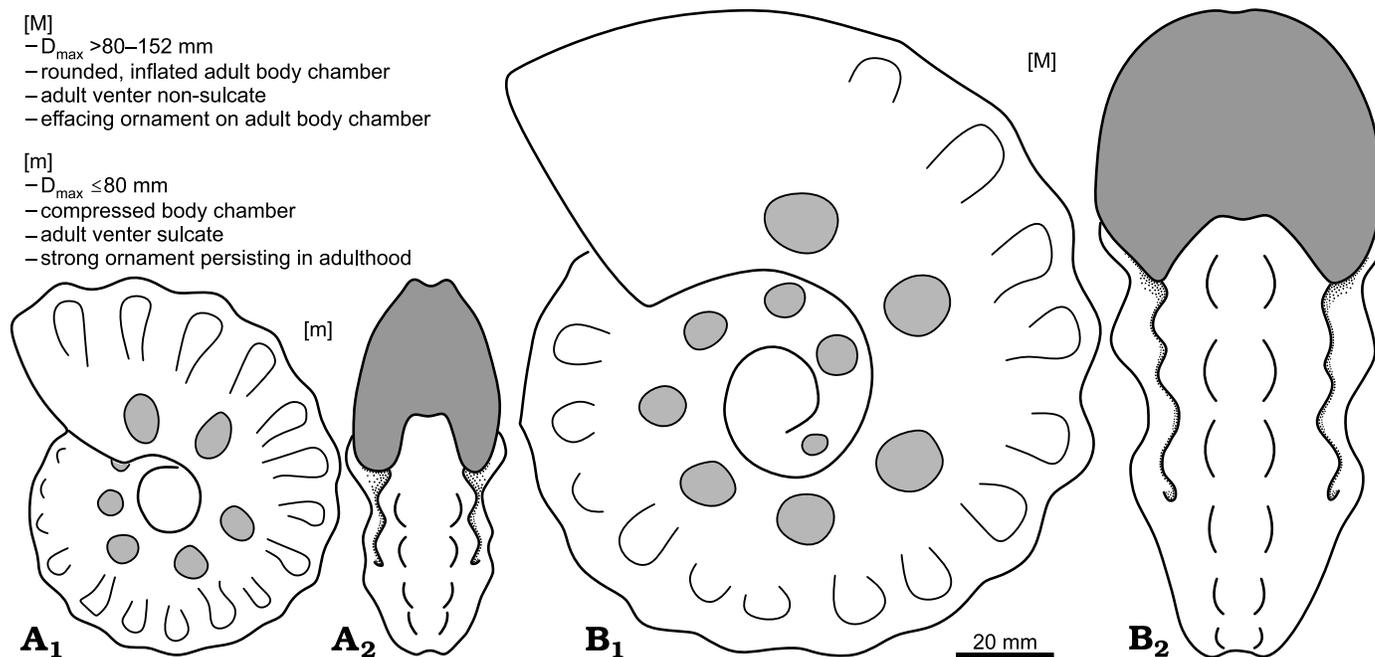
Fig. 10. Representative antidimorphs: [m] = microconch, [M] = macroconch of the acanthoceratid ammonoid *Spathites* (*Jeanrogericeras*) *reveliereanus* (Courtiller, 1860); based on (**A**) MMG: SaK 5256 in lateral (A_1) and apertural (A_2) views and (**B**) MMG: SaK 5230 in lateral (B_1) and apertural (B_2) views. Key features of both antidimorphs are listed (see text for further explanation).

ca. 100 mm (Fig. 9). However, the preservation of the inner whorls is mostly very poor. The last part of the adult body chamber in macroconchs also shows a decline in ornament (see MMG: SaK 5230 in Figs. 7A and 10 and MMG: SaK 16896 in Fig. 9) which can be, together with the change in the shape of the body chamber, regarded as a mature shell modification in ammonoids (cf. Davis et al. 1996; Klug et al. 2015c; Aiba 2022). Other signs of adulthood (e.g., septal crowding, apertural modifications) are not seen in the *S.* (*J.*) *reveliereanus* from Saxony but MMG: SaK 16500 with D = 152 mm is among the largest representatives known from this species (cf. Kennedy et al. 1980). We thus conclude for a terminal size range of 120–155 mm for fully grown macroconchs of *S.* (*J.*) *reveliereanus*.

The initially just visually suspected hypothesis of a dimorphism in *S.* (*J.*) *reveliereanus* is thus confirmed by the statistical analysis of numerous biometric parameters using two different analytical methods. Not only the maximum diameter, as in *M. nodosoides* and *L. peramplum,* but also the distinctive apertural cross-sections resulting in different Wb/Wh ratios show significant differences between the two groups (Fig. 10). In summary, it can be verified with high probability that there are two groups in the population of *S.* (*J.*) *reveliereanus* from the upper lower Turonian strata of the Brießnitz Formation, and that these two groups, based on their morphological differences, represent macro- and microconchs of a veritably dimorphic ammonite species.

Conclusions

Systematic palaeontological and biometric-statistical analyses (classical clustering and linear discriminant analysis) of statistically significant populations of three ammonite species from the upper lower Turonian strata of the Brießnitz Formation (Saxonian Cretaceous Basin, eastern Germany), i.e., *Lewesiceras peramplum* (Mantell, 1822), *Mammites nodosoides* (Schlüter, 1871) and *Spathites* (*Jeanrogericeras*) *reveliereanus* (Courtiller, 1860), were used to evaluate the formerly just visually suspected hypothesis of a size dimorphism among the taxa. Within the limitations of stratigraphic resolution, the studied faunas can in fact be regarded as contemporaneous late early Turonian assemblages (ca. 500 kyrs in duration) derived from a palaeobiogeographic entity (marly offshore deposits of the Brießnitz Formation from an area smaller than 100 km^2). Similar morphologies of small specimens and the inner whorls of larger specimens suggest more-or-less similar early ontogenies.

However, only one of three species passed the statistical tests. Neither in *M. nodosoides* nor in *L. peramplum* can a dimorphism be proven. In both taxa, no further features can be recognised that differ significantly between the size groups. Furthermore, there seem to be intermediate forms and adulthood cannot unequivocally be proven due to the absence of mature modifications. Thus, a combination of large intraspecific variability and differential preservation

that often led to incompletely preserved (i.e., small) specimens dissembles dimorphic populations at a first glance. Our results do not necessarily exclude a sexual dimorphism in in *M. nodosoides* or *L. peramplum.* They just mean that it currently cannot be substantiated by our data.

On the other hand, the suspected hypothesis of a dimorphism in *S.* (*J.*) *reveliereanus* was confirmed by the statistical analysis of numerous biometric parameters evaluated by different analytical methods. Not only the maximum diameter, as possibly in *M. nodosoides* and *L. peramplum,* but also the distinct apertural cross-sections and shapes of the venter show significant differences between the statistically clearly separated two groups. Furthermore, a decline in ornament in fully grown macroconch specimens, regarded as a mature modification of the shell, demonstrates that the antidimorphs really differed in adult morphology. Thus, it can be confirmed with high probability that there are in fact two forms in the population of *S.* (*J.*) *reveliereanus* from the upper lower Turonian of Saxony, and that these two groups, based on their morphological differences, represent micro- and macroconchs (inferred males and females) of an evidently dimorphic ammonite species.

A final conclusion is that simple visual inspection is commonly insufficient for the reliable proof of dimorphism in ammonoids.

Acknowledgements

References

Aiba, D. 2022. Dimorphism in tetragonitid ammonoid *Tetragonites minimus* from the Upper Cretaceous in Hokkaido, Northern Japan. *Acta Palaeontologica Polonica* 67: 949–961.

Amédro, F., and Delvaque, C. 2014. Les ammonites. *In*: F. Robaszynski, F. Amédro, C. Delvaque, and B. Matrion (eds.), Le Turonien des Massifs d'Uchaux et de la Cèze (S.E. France). Migration globale d'ammonites et conséquences sur la zonation internationale, rudistes et corrélations entre les massifs. *Académie royale de Belgique, Mémoires de la Classe des Sciences, Bruxelles* 4 (4): 105–164.

Arkell, W.J. 1957. Introduction to Mesozoic Ammonoidea. *In*: W.J. Arkell, W.M. Furnish, B. Kummel, A.K. Miller, R.C. Moore, O.H. Schindewolf, P.C. Sylvester-Bradley, and C.W. Wright (eds.), *Treatise on Invertebrate Paleontology, Part L, Mollusca 4*, L81–L129. Geological Society of America and University of Kansas Press, Lawrence.

Balakrishnama, S. and Ganapathiraju, A. 1998. *Linear Discriminant Analysis. A Brief Tutorial.* 8 pp. Institute for Signal and Information Processing, Department of Electrical and Computer Engineering, Mississippi State University, Starkville.

Beck, R. and Hazard, J. 1892. *Geologische Specialkarte des Königreichs Sachsen. Section Dresden 66*. W. Engelmann, Leipzig.

Beck, R. and Hazard, J. 1893. Erläuterungen zur geologischen Specialkarte des Königreichs Sachsen. *Section Dresden 66*. 102 pp. W. Engelmann, Leipzig.

Beeger, H.D. 1963. Die petrographische Ausbildung und die Obergrenze des Labiatus–Sandsteins im Gebiet von Pirna und Königstein. *Berichte der Geologischen Gesellschaft in der Deutschen demokratischen Republik* 8: 205–213.

Callomon, J.H. 1963. Sexual dimorphism in Jurassic ammonites. *Transactions of the Leicester Literary and Philosophical Society* 57: 21–56.

Cobban, W.A. 1969. The Late Cretaceous ammonites *Scaphites leei* Reeside and *Scaphites hippocrepis* (DeKay) in the Western Interior of the United States. *United States Geological Survey Professional Paper* 619: 1–27.

Cobban, W.A. and Kennedy, W.J. 1993. The Upper Cretaceous dimorphic pachydiscid ammonite *Menuites* in the Western Interior of the United States. *U.S. Geological Survey Professional Paper* 1533: 1–14.

Courtiller, M.A. 1860. Description de trois nouvelles espèces d'ammonites du terrain crétacé. *Mémoire de la Société impériale d'Agriculture, Science et des Arts d'Angers* 3: 246–252.

Davis, R.A. 1972. Mature modification and dimorphism in selected late Paleozoic ammonoids. *Bulletin of American Paleontology* 62: 23–130.

Davis, R.A., Landman, N.H., Dommergues, J.L., Marchand D., and Bucher H. 1996. Mature modifications and dimorphism in ammonoid cephalopods. *In*: N.H. Landman, K. Tanabe, and R.A. Davis (eds.), Ammonoid Paleobiology. *Topics in Geobiology* 13: 463–539.

De Blainville, M.H.D. 1840. *Prodrome d'une monographie des ammonites. Supplément du Dictionnaire des Sciences Naturelles*. 31 pp. Bertrand, Paris.

De Grossouvre, A. 1894. Recherches sur la Craie supérieure. Deuxième part: Paléontologie. Les ammonites de la Craie supérieure. *Mémoires pour servir à l'explication de la carte géologique détaillée de la France*. 264 pp. Imprimerie nationale, Paris.

Elmi, S. 1993. Area-rule, boundary layer and functional morphology of cephalopod shells (ammonoids). *Geobios* 15: 121–138.

Gale, A.S., Mutterlose, J., and Batenburg, S. with contributions by Gradstein, F.M., Agterberg, F.P., Ogg, J.G., and Petrizzo, M.R. 2020. The Cretaceous Period. *In*: F.M. Gradstein, J.G. Ogg, M.D. Schmitz, and G.M. Ogg (eds.), *Geologic Time Scale 2020, Volume 2*, 1023–1086. Elsevier, Amsterdam.

Guex, J. 1970. Sur les moules internes des Dactyliocératides. Musee Geologique de L'Universite de Lausanne. *Bulletin de la Société Vaudoise des Sciences Naturelles* 70 (182): 1–7.

Hammer, Ø., Harper, D.A.T., and Ryan, P.D. 2001. Past: Paleontological Statistics Software Package for Education and Data Analysis. *Palaeontologia Electronica* 4 (1): 1–9.

Hanlon, R.T. 1982. The functional organization of chromatophores and iridescent cells in the body patterning of *Loligo plei* (Cephalopoda, Myopsida). *Malacologia* 23: 89–119.

House, M.R. 1989. Ammonoid extinction events. *Philosophical Transactions of the Royal Society B: Biological Sciences* 325: 307–326.

Hyatt, A. 1889. Genesis of the Arietidae. *Smithsonian Contributions to Knowledge* 673: i–xi, 1–238.

Hyatt, A. 1900. Cephalopoda. *In*: K.A. von Zittel (ed.), *Textbook of Palaeontology* (translated by C.R. Eastman), 502–592. Macmillan, London.

Janetschke, N. and Wilmsen, M. 2014. Sequence stratigraphy of the lower Upper Cretaceous Elbtal Group (Cenomanian–Turonian of Saxony, Germany). *Zeitschrift der Deutschen Gesellschaft für Geowissenschaften* 165: 179–208.

Jattiot, R., Lehmann, J., Kruta, I., and Rouget, I. 2023. Mature modifications and sexual dimorphism in Turrilitidae (heteromorph ammonites): Contribution of remarkable *Mariella bergeri* specimens (upper Albian, southeastern France). *Cretaceous Research* 151: 105651.

Johnson, S.C. 1967. Hierarchical clustering schemes. *Psychometrika* 32: 241–254.

Kennedy, W.J. 1989. Thoughts on the evolution and extinction of Cretaceous ammonites. *Proceedings of the Geologists' Association* 100: 251–279.

Kennedy, W.J. and Cobban, W.A. 1976. Aspects of ammonite biology, biogeography, and biostratigraphy. *Special Papers in Palaeontology* 17: 1–94.

Kennedy, W.J. and Gale, A.S. 2016. Turonian ammonites from northwestern Aquitaine, France. *Cretaceous Research* 58: 265–296.

Kennedy, W.J. and Kaplan, U. 2019. Ammoniten aus dem Turonium des Münsterländer Kreidebeckens. *Geologie und Paläontologie in Westfalen* 92: 3–223.

Kennedy, W.J., Wright, C.W., and Hancock, J.M. 1980. Origin, evolution, and systematics of the Cretaceous ammonite *Spathites. Palaeontology* 23: 821–837.

Keupp, H. 2000. *Ammoniten. Paläobiologische Erfolgsspiralen*. 165 pp. Thorbecke, Stuttgart.

Kirenz, J. 2020. *Hierarchische Clusteranalyse mit Ward in R*; available at https://www.kirenz.com/post/2020-05-21-r-hierarchische-clusteranalyse/ (accessed 28.08.2020).

Klug, C., Korn, D., De Baets, K., Kruta, I., and Mapes, R.H. (eds.) 2015a. Ammonoid Paleobiology: From Anatomy to Evolution. *Topics in Geobiology* 43: i–xxv, 1–934.

Klug, C., Korn, D., De Baets, K., Kruta, I., and Mapes, R.H. (eds.) 2015b. Ammonoid Paleobiology: From Macroevolution to Paleogeography. *Topics in Geobiology* 44: i–xxi, 1–605.

Klug, C., Zatoń, M., Parent, H., Hostettler, B., and Tajika, A. 2015c. Mature modifications and sexual dimorphism. *In*: C. Klug, D. Korn, K. De Baets, I. Kruta, and R.H. Mapes (eds.), Ammonoid Paleobiology: From Anatomy to Ecology. *Topics in Geobiology* 43: 253–320.

Kummel, B. and Decker, J.M. 1954. Lower Turonian ammonites from Texas and Mexico. *Journal of Paleontology* 28: 310–319.

Landman, N.H. and Waage, K.M. 1993. Scaphitid ammonites of the Upper Cretaceous (Maastrichtian) Fox Hills Formation in South Dakota and Wyoming. *Bulletin of the American Museum of Natural History* 215: 1–257.

Landmann, N.H., Klofak, S.M., and Sarg, K.B. 2008. Variation in adult size of scaphitid ammonites from the Upper Cretaceous Pierre Shale and Fox Hills Formation. *In*: P.J. Harries (ed.), High-Resolution Approaches in Stratigraphic Paleontology. *Topics in Geobiology* 21: 149–194.

Landmann, N.H., Tanabe, K., and Davis, R.A. (eds.) 1996. Ammonoid Paleobiology. *Topics in Geobiology* 13: i–xxiv, 1–857.

Laube, G.C. and Bruder, G. 1887. Ammoniten der böhmischen Kreide. *Palaeontographica* 33: 217–239.

Laurin, J., Uličny, D., Čech, S., Trubač, J., Zachariaš, J., and Svobodova, A. 2021. Chronology and eccentricity phasing for the Early Turonian greenhouse (~93–94 Ma): Constraints on astronomical control of the carbon cycle. *Paleoceanography and Paleoclimatology* 36 (4): e2020PA004188.

Lehmann, U. 1966. Dimorphismus bei Ammoniten der Ahrensburger Lias-Geschiebe. *Paläontologische Zeitschrift* 40: 26–55.

Lehmann, U. 1976. *Ammoniten: Ihr Leben und ihre Umwelt*. 173 pp. Ferdinand Enke Verlag, Stuttgart.

Lehmann, U. 1981. Ammonite jaw apparatus and soft parts. *In*: M.R. House and J.R. Senior (eds.), *The Ammonoidea*, 275–287. Academic Press, London.

Machalski, M. 2005. Late Maastrichtian and earliest Danian scaphitid ammonites from central Europe: Taxonomy, evolution, and extinction. *Acta Palaeontologica Polonica* 50: 653–696.

Maeda, H. 1993. Dimorphism of Late Cretaceous false-puzosiine ammonites, *Yokoyamaoceras* Wright and Matsumoto, 1954 and *Neopuzosia* Matsumoto, 1954. *Transactions and Proceedings of the Palaeontological Society of Japan, New Series* 169: 97–128.

Makowski, H. 1962. Problem of sexual dimorphism in ammonites. *Palaeontologia Polonica* 12: 1–92.

Mantell, G.A. 1822. *The Fossils of the South Downs, or Illustrations of the Geology of Sussex*. xiv + 328 pp., 43 pls. Lupton Relfe, London.

Matrion, B. 2018. Les ammonites. *In*: F. Amédro, B. Matrion, and F. Robaszynski (eds.), Stratotype Turonien. *Patrimoine Géologique* 8: 183–244.

Matyja, B.A. 1986. Developmental polymorphism in Oxfordian ammonites. *Acta Geologica Polonica* 36: 37–38.

Monnet, C., De Baets, K., and Klug, C. 2011. Parallel evolution controlled by adaptation and covariation in ammonoid cephalopods. *BMC Evolutionary Biology* 11 (115): 1–21.

Munier-Chalmas, E.C.P.A. 1892. Sur le possibilitié d'admettre un dimorphisme sexuel chez les ammonitides. *Bulletin de la Societé Geologique de France, Comptes Rendus III* 25: 170–174.

Niebuhr, B. and Wilmsen, M. 2023. The transgression history of the Saxonian Cretaceous revisited or: the imperative for a complete stratigraphic reappraisal (Cenomanian, Elbtal Group, Germany). *Zeitschrift der deutschen Gesellschaft für Geowissenschaften* 174: 69–118.

Niebuhr, B., Hiss, M., Kaplan, U., Tröger, K.-A., Voigt, S., Voigt, T., Wiese, F., and Wilmsen, M. 2007. Lithostratigraphie der norddeutschen Oberkreide. *Schriftenreihe der Deutschen Gesellschaft für Geowissenschaften* 55: 1–136.

Niebuhr, B., Wilmsen, M., and Voigt, T. 2020. Die Oberkreide (Cenomanium–Mittelconiacium) im Zittauer Sandsteingebirge (Deutschland, Tschechien). *Zeitschrift der deutschen Gesellschaft für Geowissenschaften* 171: 163–197.

Palframan, D.F.B. 1966. Variation and ontogeny of some Oxfordian ammonites: *Taramelliceras richei* (De Loriol) and *Creniceras renggeri* (Oppel), from Woodham, Buckinghamshire. *Palaeontology* 9: 290–311.

Palframan, D.F.B. 1967. Variation and ontogeny of some Oxford Clay ammonites: *Distichoceras bicostatum* (Stahl) and *Horioceras baugieri* (d'Orbigny), from England. *Palaeontology* 10: 60–94.

Parent, H. and Zatoń, M. 2016. Sexual dimorphism in the Bathonian morphoceratid ammonite *Polysphinctites tenuiplicatus*. *Acta Palaeontologica Polonica* 61: 875–884.

Raschka, S. 2014. *Linear Discriminant Analysis—Bit by Bit*; available at https://sebastianraschka.com/Articles/2014_python_lda.html (accessed 02.09.2020).

Richardt, N., Wilmsen, M., and Niebuhr, B. 2013. Late Cenomanian–Early Turonian facies development and sea-level changes in the Bodenwöhrer Senke (Danubian Cretaceous Group, Bavaria, Germany). *Facies* 59: 803–827.

Ritterbush, K.A., Hoffmann, R., Lukeneder, A., and De Baets, K. 2014. Pelagic palaeoecology: the importance of recent constraints on ammonoid palaeobiology and life history. *Journal of Zoology* 292: 229–241.

Schlüter, C.A. 1871. Cephalopoden der oberen deutschen Kreide. 1. Abtheilung. Lieferung 1. *Palaeontographica* 21: 1–24, pls. 1–8.

Spath, L.F. 1922. On the Senonian ammonite fauna of Pondoland. *Transactions of the Royal Society of South Africa* 10: 113–148.

Spath, L.F. 1939. Problems of ammonite nomenclature. The genus *Pachydiscus* Zittel. *Geological Magazine* 76: 293–296.

Tanabe, K. 2022. Late Cretaceous dimorphic scaphitid ammonoid genus *Yezoites* from the circum-North Pacific regions. *Paleontological Research* 26: 233–269.

Tröger, K.-A. 1988. Zur Bio- und Lithostratigraphie der Brießnitzer Schichten bei Dresden. *Freiberger Forschungshefte C* 419: 89–95.

Tsujita, C.J. and Westermann, G.E.G. 1998. Ammonoid habitats and habits in the Western Interior Seaway: a case study from the Upper Cretaceous Bearpaw Formation of southern Alberta, Canada. *Palaeogeography, Palaeoclimatology, Palaeoecology* 144: 135–160.

Voigt, T. 1999. Ablagerungsbedingungen und Taphonomie der Schmilka-Formation (Unter-Turon) südlich von Pirna (Sächsisches Kreidebecken). *Greifswalder Geowissenschaftliche Beiträge* 6: 193–207.

Vollrath, F. 1998. Dwarf males. *Trends in Ecology and Evolution* 13: 159–163.

Ward, P.D. 1979. Functional morphology of Cretaceous helically-coiled ammonite shells. *Paleobiology* 5: 415–422.

Ward, P.D. 1987. *The Natural History of Nautilus*. 267 pp. Allen and Unwin, London.

Ward, P.D., Dooley, F., and Barord, G.J. 2016. *Nautilus*: biology, systematics, and paleobiology as viewed from 2015. *Swiss Journal of Palaeontology* 135: 169–185.

Westermann, G.E.G. 1964. Sexual-Dimorphismus bei Ammonoideen und seine Bedeutung für die Taxionomie der Otoitidae (einschließlich Sphaeroceratinae; Ammonitina, M. Jura). *Palaeontographica A* 124 (1–3): 33–73.

Westermann, G.E.G. 1996. Ammonoid life and habitat. *In*: N.H. Landman, K. Tanabe, and R.A. Davis (eds.), Ammonoid Paleobiology. *Topics in Geobiology* 13: 607–707.

Wiedmann, J. 1960. Le Crétacé supérieur de l'Espagne et du Portugal et ses céphalopodes. *In*: *Comptes Rendus du Congrès des Sociétés Savantes-Dijon, 1959. Colloque sur le Crétacé supérieur français*, 709–764. [misdated 1959]

Wiese, F., Cech, S., Ekrt, B., Kost'ak, M., Mazuch, M., and Voigt, S. 2004. The Upper Turonian of the Bohemian Cretaceous Basin (Czech Republic) exemplified by the Ùpholavy working quarry: integrated stratigraphy and palaeoceanography of of a gateway to the Tethys. *Cretaceous Research* 25: 329–352.

Wilmsen, M. 2016. Nautiliden. *In*: B. Niebuhr and M. Wilmsen (eds.), Kreide-Fossilien in Sachsen, Teil 2. *Geologica Saxonica* 62: 59–102.

Wilmsen, M. and Nagm, E. 2013. Upper Cenomanian–Lower Turonian ammonoids from the Saxonian Cretaceous (lower Elbtal Group, Saxony, Germany). *Bulletin of Geosciences* 88: 647–674.

Wilmsen, M. and Nagm, E. 2014. Ammoniten. *In*: B. Niebuhr and M. Wilmsen (eds.), Kreide-Fossilien in Sachsen, Teil 1. *Geologica Saxonica* 60: 201–240.

Wilmsen, M. and Niebuhr, B. 2014. Die Kreide in Sachsen. *In*: B. Niebuhr and M. Wilmsen (eds.), Kreide-Fossilien in Sachsen, Teil 1. *Geologica Saxonica* 60: 3–12.

Wilmsen, M., Niebuhr, B., and Kennedy, W.J. 2022. Middle Cenomanian ammonites from the Oberhäslich Formation (Elbtal Group, Germany): stratigraphic and palaeogeographic implications for the Saxo-Bohemian Cretaceous. *Neues Jahrbuch für Geologie und Paläontologie Abhandlungen* 303: 271–294.

Wilmsen, M., Niebuhr, B., Fengler, M., Püttmann, T., and Berensmeier, M. 2019. The Late Cretaceous transgression in the Saxonian Cretaceous Basin (Germany): old story, new data and novel findings. *Bulletin of Geosciences* 94: 71–100.

Wilmsen, M., Wondrejz, C., Püttmann, T., and Kennedy, W.J. 2021. *Cibolaites petraschecki* sp. nov., a new collignoniceratine ammonite from the Brießnitz Formation of Saxony (Turonian, Elbtal Group, Germany). *Neues Jahrbuch für Geologie und Paläontologie Abhandlungen* 300: 187–197.

Wondrejz, C. 2021. *Taxonomy, Palaeobiology and Palaeoecology of the Early Turonian Ammonite Assemblage of the Brießnitz Formation in the Dresden Area (Elbtal Group, Saxony)*. 99 pp. + Appendix 53 pp. Unpublished M.Sc. Thesis, TU Dresden, IHI Zittau, Dresden.

Wright, C.W. and Kennedy, W.J. 1981. The Ammonoidea of the Plenus Marls and the Middle Chalk. *The Palaeontographical Society Monograph* 560: 1–148.

Wright, C.W. and Kennedy, W.J. 1984. The Ammonoidea of the Lower Chalk. Part 1. *The Palaeontographical Society Monograph* 567: 1–126.

Zittel, K.A. 1895. *Grundzüge der Paläontologie*. viii + 971 pp. Oldenbourg, München.